DTU Library

Effects on the structure of monolayer and submonolayer fluid nitrogen films by the corrugation in the holding potential of nitrogen molecules

Hansen, Flemming Yssing

Link back to DTU Orbit

Effects on the structure of monolayer and submonolayer fluid nitrogen films by the corrugation in the holding potential of nitrogen molecules

F. Y. Hansen
Department of Chemistry, Technical University of Denmark, IK 207 DTU, DK-2800, Lyngby, Denmark

Molecular dynamics simulations have been used to study the effects of the corrugation in the holding potential of nitrogen molecules on the structure of fluid monolayer and submonolayer films of the molecules on a solid substrate. Structures of monolayer and submonolayer fluid films of nitrogen molecules adsorbed on graphite and on a model uncorrugated "smooth" graphite surface are compared. For films on the "smooth" graphite surface the melting temperature is lowered by 7 K. Contrary to what is found for films on the corrugated surface, the simulations show that there is a region of liquid–gas coexistence, demonstrating that this is a normal triple point system. A discrepancy between calculated and experimental melting temperatures of submonolayer films was traced to the intermolecular potentials. These have been tested by comparing molecular dynamics simulations of isosteric heats of adsorption in fluid films with experimental measurements. The establishment of the effects of the corrugation in the holding potential on the structure provides a basis for the study of the effects on the dynamical excitations in the films. © 2001 American Institute of Physics. [DOI: 10.1063/1.1380372]

I. INTRODUCTION

Over the past years, there have been several theoretical studies[1–4] of the physisorption of nitrogen molecules on the basal planes of graphite. The system has also been studied extensively by a variety of experimental techniques[5] such as elastic and inelastic neutron scattering, x-ray scattering, calorimetry, and adsorption isotherms; it may therefore be considered as a "benchmark" case for diatomic molecules physisorbed on the basal planes of graphite and is accordingly suitable for detailed theoretical studies. Subsequent experiments with electron diffraction[6,7] and helium atom[8,9] scattering for nitrogen physisorbed on metal surfaces have shown similarities with the graphite results and differences in the occurrence of commensurate structures. Most of these studies are for solid films of nitrogen, but the recent extensions of quasielastic neutron[10] and helium atom[11] scattering experiments may make it possible to obtain data for the dynamics of the fluid phases as well.

In another paper[12] we present detailed studies and predictions of how the corrugation in the potential influences the dynamic excitations in fluid films of nitrogen including translational and rotational diffusive motions and the possibilities of observing these by quasielastic neutron scattering and helium atom scattering. As a basis for such studies and for the validation of the predictions, it is important to establish how our model of the system describes the structure of the system and in particular how the corrugation influences the structure. That is the purpose of this paper.

A systematic study of the fluid phase also has a broader interest. The N_2/graphite system is an incipient triple-point system,[13] in which the corrugation of the holding potential apparently causes the triple-point temperature to be higher than the critical temperature of gas–liquid coexistence. Simulations of N_2/Ag(111) showed[14] that N_2 on a smooth surface is a normal triple-point system and this is also the case in the present simulation for "smooth" graphite. The structure of the fluid is modulated by the corrugation, so that the "rings" of a diffraction pattern on a smooth surface become "spotty rings" of a lattice fluid on the corrugated surface.

The recent theoretical investigations have primarily been based on molecular dynamics (MD) and Monte Carlo (MC) simulations of the monolayer and submonolayer systems. In one series of studies,[3] the corrugation in the holding potential has been analyzed, and it was found that the commonly used empirical potential[15] underestimated the corrugation. The agreement with experiments was improved when the asymmetric charge distribution in graphite was included in the interaction model.

Another series of studies,[4] have been focused on the melting transition in monolayer and submonolayer films. It was shown that the melting mechanism in monolayer films and submonolayer films is quite different. In the former, the melting transition is initiated by molecules moving up to the second layer thereby creating space in the first layer for the translational order to break down, while in submonolayer films vacancies move in from the edge regions of the film. The activation energies associated with these processes are quite different, hence the large difference in melting temperatures between monolayer and submonolayer films.

In monolayer films, the melting temperature is mainly determined by the average holding potential, and the good agreement between calculated and experimental melting temperature indicates that the representation of that part of the potential is fairly good.

In submonolayer films, a rather large discrepancy was found between calculated and experimental melting temperature. The calculations gave a melting temperature of ∼34 K

as compared to the experimental melting temperature of ~47 K. Based on our understanding of the submonolayer melting mechanism, the origin of this discrepancy should be sought in the lateral part of the holding potential and in the intermolecular potentials. The former was checked by simulations and inelastic neutron scattering measurements as mentioned above.[3] The intermolecular interactions are in our model made up of three contributions: (a) a Lennard-Jones atom–atom contribution; (b) a molecular quadrupole–quadrupole interaction; and (c) the McLachlan mediation of the interatomic interactions due to the polarizability of the electrons in the graphite substrate. The former two interactions are based on models for a nitrogen solid and fluid, and the latter is based on a perturbation treatment by McLachlan.[16] The McLachlan interaction energy E_{ij}^{McL} between adsorbed atoms i and j is given by

$$E_{ij}^{McL} = \frac{CS1}{(R_{ij}R_{i'j})^3}$$
$$\times \left[\frac{4}{3} - \frac{(r_{jz}+r_{iz}-zlay)^2}{R_{i'j}^2} - \frac{(r_{jz}-r_{iz})^2}{R_{ij}^2} \right] - \frac{CS2}{R_{i'j}^6}, \quad (1)$$

with $CS1 = 5.7898 \times 10^4$ K Å^6 and $CS2 = 2.9468 \times 10^4$ K Å^6.[16] i' is the image of atom i in a mirror plane parallel to the surface and shifted $zlay/2$ outwards, where $zlay = 3.37$ Å is the distance between the basal planes in graphite. R_{ij} and $R_{i'j}$ are the distances between adsorbed atoms i and j and between i', the image of atom i, and j. r_{jz} and r_{iz} are the z coordinates of atoms j and i. For atoms at the same distance from the surface this term weakens the intermolecular interactions. Good agreement with the experimental melting point was found, if the McLachlan term was reduced from being ~15% of the intermolecular potential to only a few percent. An important parameter in the expression for the McLachlan mediation term is the position of the mirror plane for the image charges in graphite with respect to the physical surface. It has to be changed quite drastically from the commonly accepted position which is half the distance between basal planes outside the physical surface. Alternatively, one could imagine that a term in the intermolecular potential is missing, which could offset the contribution from the mediation term. Another independent check of the intermolecular potentials is offered by the isosteric heat of adsorption which has been determined experimentally for the fluid phase at 79.3 K,[17] and is exploited in this paper.

The interaction model and the isothermal constrained dynamics algorithm are the same as in our previous papers.[3,18] The submonolayer patches are in the form of stripes as described in Ref. 3. A complete monolayer has 224 molecules in the simulation cell and the densities are given as fractions (e.g., $\rho = 7/14$) of a commensurate monolayer density $\rho = 1$ for graphite, 0.0636 Å^2. In the simulation of systems at and near monolayer completion, promotion of molecules from the first layer to the second layer and to the 3D gas phase becomes important. To ensure equilibration, molecules in the 3D gas phase are reflected elastically when they reach a distance of 12 Å from the surface. At that distance the interactions between molecule and substrate are practical zero. The propagation times for these systems are quite long to ensure a proper equilibration and typically in the range of 1500–2000 ps; other systems are typically propagated for ≈800–1000 ps. The organization of the paper is as follows: In Sec. II the effect of the corrugation in the holding potential on the structure of the fluid is discussed, including a discussion of the incipient triple point system; in Sec. III, we describe the calculations of the isosteric heat of adsorption and compare the results to the experimental results. Section IV has some concluding remarks.

II. STRUCTURE OF THE FLUID FILMS

A. Incipient triple point system

The melting temperature of submonolayer N$_2$/graphite is nearly constant over a wide range of intermediate coverages[19] around $\rho = 7/14$, where $\rho = 1$ for a perfect commensurate monolayer. To parallel this, our most detailed determination of the melting temperature on the model uncorrugated, "smooth" graphite surface is for the $\rho = 7/14$ film. As in previous work,[3] we calculated the intermolecular potential energy and the (1,1) structure factor as a function of temperature and took the melting temperature to be the temperature at the inflection points of those curves. However, in the calculations of the submonolayer on the "smooth" graphite we could not use the (1,1) structure factor directly, since the patch rotated slightly on the substrate. On a corrugated surface, the patch is locked in and does not rotate. Instead we used the spherical-averaged structure factor, which is unaffected by a slight rotation of the patch on the surface.

An inflection point is evident at ≈27 K in Fig. 1(a), although it is not as prominent as in the corrugated-surface simulations. The height of the major (1,1) diffraction peak in the spherical-averaged structure factor, shown in Fig. 1(b), also has an inflection point at ≈27 K. This value for the melting temperature of the submonolayer is close to the range 27.5–30 K for the triple-point temperature set[14] by using the criterion of the onset of a van der Waals loop at nearly zero pressure. The melting temperature is 7 K lower than the 34 K calculated with the same molecular interactions (denoted X1M) on the corrugated graphite surface. This is consistent with the submonolayer mechanism of melting, where vacancies move into the patch from the edge regions, so the melting point is determined by the lateral interactions in the film. At all submonolayer coverages considered here, the melting point dropped by 7 K with a model uncorrugated graphite surface compared to the ordinary graphite surface.

The agreement between the melting temperature on the "smooth" surface for $\rho = 7/14$ and the triple-point temperature determined[14] for a homogeneous cell of 224 molecules shows that finite-size effects are still small for the 112-molecular computational cell. However the 22 K melting temperature for $\rho = 3/14$ on the smooth surface, with 48 molecules in the cell, is distinctly lower and shows finite-size effects.

Based on Landau free energy calculations,[13] it has been suggested that the nitrogen–graphite system is a so-called incipient triple point system, where the triple point temperature has been shifted upwards thanks to the corrugation, so it
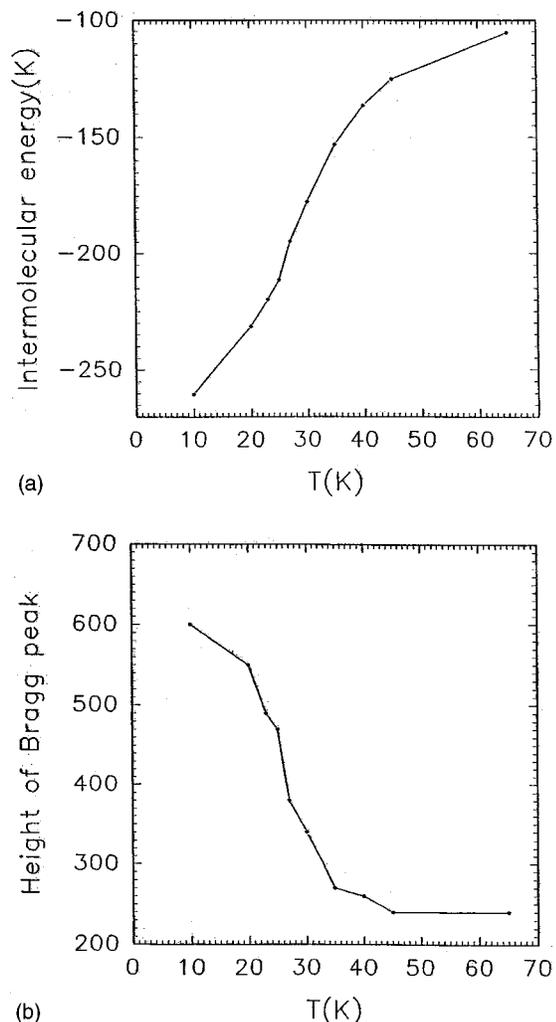
FIG. 1. Determination of the melting temperature for the $\rho=7/14$ film on a model uncorrugated graphite surface. (a) The intermolecular potential energy per molecule as function of temperature. (b) The intensity of the major (1,1) peak in the spherical averaged structure factor.

is higher than the critical temperature. The effect of the corrugation is simply to extend the temperature region of the solid phase. When the film finally melts, a fluid phase is formed, where the molecules are distributed over the available surface rather than forming a dense self-bound liquid phase in equilibrium with a 2D gas phase. This proposition has been tested in the simulations.

In Fig. 2(a) is seen a 200 ps trajectory plot for the $\rho=0.5$ monolayer system on a model uncorrugated graphite surface at 30 K, just 3 K above the melting temperature and 4 K below the melting temperature on a corrugated surface. The center-of-mass positions of the nitrogen molecules have been plotted every 4.5 ps and the positions have been connected by straight lines. The lines do therefore not represent true trajectories. In a normal triple point system, we should see the patch being disordered but holding together with a few trajectories extending into the 2D gas phase. The figure clearly shows that the patch holds together and that it is disordered. For comparison we have shown in Fig. 2(b) the results for a film on a corrugated surface at 35 K, just 1 K above the melting point. Here we see that the molecules are

spread out over the entire surface contrary to what was seen for the smooth surface system. The obvious large fluctuations in the density indicate that we are close to the critical point. Already at 40 K, the fluctuations are much less pronounced. Another striking example of a self-bound liquid state is shown in the trajectory plot Fig. 3(a) for average coverage $\rho=3/14$ on the "smooth" graphite surface at 25 K, 3 K above its melting point. In Fig. 3(b) is shown the trajectory plot for the same system on a corrugated surface at 30 K, 1 K above the melting temperature, and it is seen that the patch breaks up. The fluctuations are so pronounced here that there even are solid like regions in the patch.

We have constructed trajectory plots for $\rho=3/14$, $7/14$, and $10/14$ on the smooth surface at 30, 35, and 40 K. For all three densities, the trajectories indicate a self-bound liquid state at 30 K and uniform gas at 40 K, while 35 K is an intermediate case with complex clustering. On this basis, we estimate the critical temperature for gas–liquid coexistence is near 35 K.[20]

Another diagnostics we have used is a calculation of the pair distribution function $g(r)$. In the simulation the average number of molecules $n(r)$ at a distance r from a molecule is monitored. The data are binned into bins of width δr. The relation between $n(r)$ and $g(r)$ is given by

$$n(r) = 2\pi r g(r)\rho_0 \delta r, \tag{2}$$

where ρ_0 is the average density, that is the number of molecules in the simulation box divided by its area. Clearly, if the molecules form a dense liquid patch, with only a few molecules in the 2D gas phase, then the ρ_0 normalization will only be $\approx$ half the density in the liquid phase for a system with $\rho=0.5$. On this basis we should expect that the limiting value of $g(r)$ at large distances will approach the value of 2 rather than the usual value of 1. In practice, however, edge effects obscure that picture. As r is increased, there will be molecules in fewer and fewer directions around a given molecule. In most directions there will be empty space from the free area between patches in the y-direction. So one should expect a $g(r)$ function which will be larger at intermediate distances due to the effectively higher density in the liquid phase, but then becomes smaller as more and more free space will be included in the calculation resulting in a limiting value which eventually may be smaller than 1. These features may be seen in Fig. 4(a), where we have plotted the $g(r)$ function at different temperatures out to 20 Å for the $\rho=7/14$ system on a smooth surface. The data seems indeed to be significantly larger at 30 K than at the other temperatures above the critical point. This supports the conclusion that it is a normal triple point system, when the corrugation in the holding potential is eliminated. As a comparison, we have shown the results for the corrugated surface in Fig. 4(b), where the effect of the normalization is smaller as expected since the fluid phase fills the entire simulation box.

Based on the discussion above, the pair distribution function is not a good diagnostics for distinguishing between a fluid system and a two phase liquid/2D gas system. At higher coverages, the difference in density also becomes smaller such that it is impossible to distinguish between the
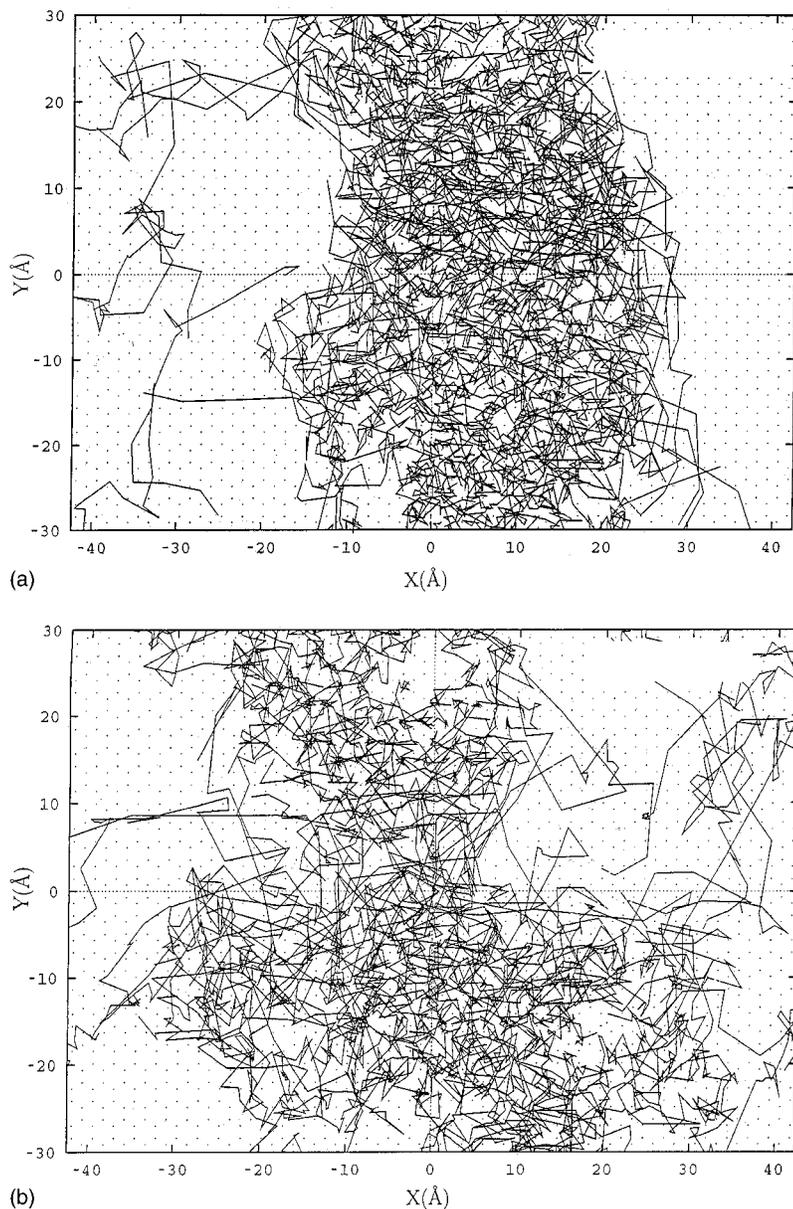
FIG. 2. Trajectory plots of the $\rho=0.5$ film on a model uncorrugated graphite surface and a corrugated graphite surface. The dots forming a hexagonal pattern show the carbon atom positions in the graphite. (a) Model uncorrugated graphite surface at 30 K, 3 K above the melting temperature. (b) Corrugated graphite surface at 35 K, just 1 K above the melting temperature.

two types of phases; on the other hand, trajectory plots are very useful at smaller coverages as demonstrated in Fig. 3(a).

In summary, systems at low coverages should be used to test whether the system is a normal triple point system or an incipient triple point system. In our simulations we have found evidence for the prediction that the N_2/graphite system indeed is an incipient triple point system caused by the corrugation in the holding potential, and when the corrugation is removed, it becomes a normal triple point system.

B. 2D structure factor of the fluid films

In order to make connection to possible experimental observations of the fluid film surface, we have determined the 2D structure factor of the fluid films at various coverages as a function of the temperature. The structure factor is proportional to the intensity in a scattering experiment and given by the expression,

$$S(\mathbf{q}) = \left\langle \left| \sum_{j=1}^{N} \sum_{\alpha=1}^{2} \exp(i\mathbf{q} \cdot \mathbf{R}_{j\alpha}) \right|^2 \right\rangle, \tag{3}$$

where $\mathbf{R}_{j\alpha}$ is the position vector of atom α in the jth molecule and $\mathbf{q}$ is the wave vector; the average is taken over a 200 ps time sequence. This is an idealized version of a LEED pattern of an adlayer on a single crystal surface. The translational order of a crystal is manifested as a spot pattern in the intensity while the fluid has a series of rings. Three examples of $S(\mathbf{q})$ for the $\rho=10/14$ average coverage are shown in Fig. 5. In (a) for the corrugated surface at 35 K, there are intense spots at the locations of the six 1.70 Å^{-1} reciprocal lattice vectors of the commensurate solid, only slightly smeared in the azimuthal angle, and a weak ring of intensity. There also are four intense N_2 spots at $\approx(\pm 2.6, \pm 1.5)$ Å^{-1}, which are positions of the 2.95 Å^{-1} graphite reciprocal lattice vectors. The combination of a ring and a spot pattern shows the strong influence of the corrugation[21] on the struc-
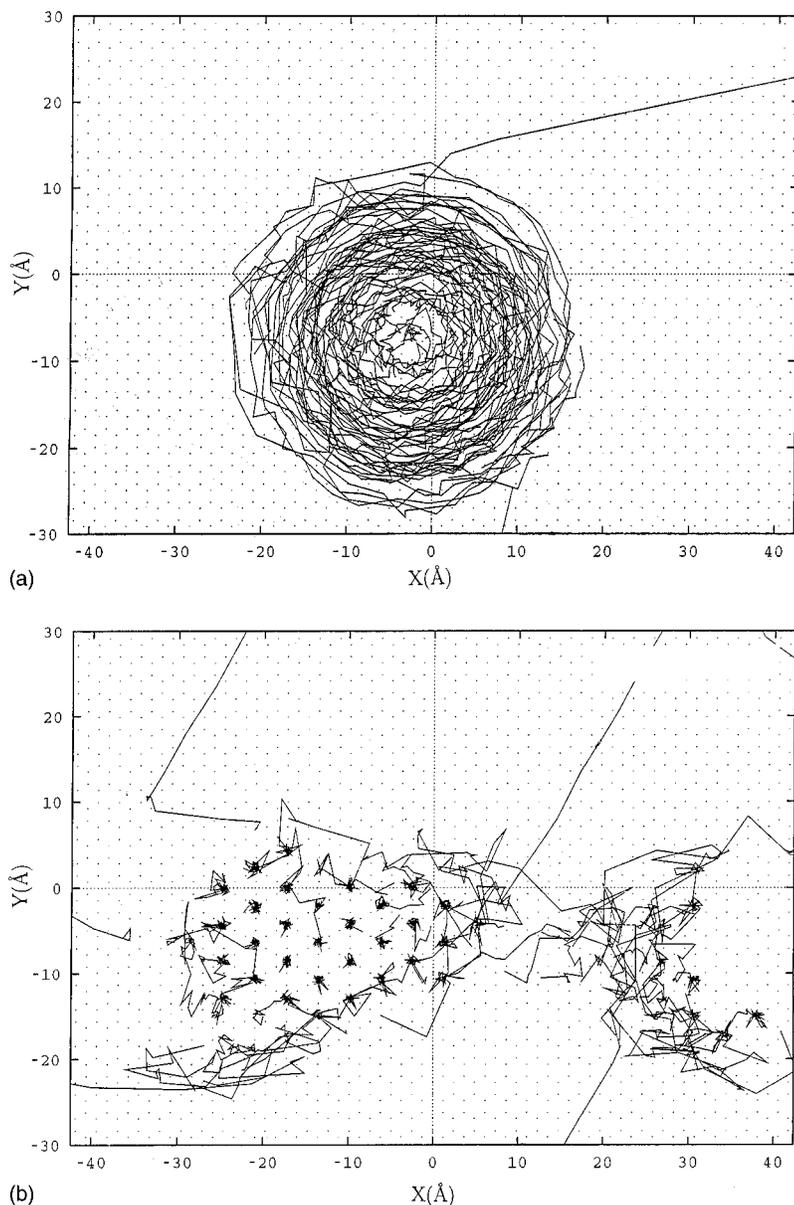
FIG. 3. Trajectory plots of the $\rho=3/14$ film on a model uncorrugated graphite surface and a corrugated graphite surface. The dots forming a hexagonal pattern show the carbon atom positions in the graphite. (a) Model uncorrugated graphite surface at 25 K, 3 K above the melting temperature. (b) Corrugated graphite surface at 35 K, 3 K above the melting temperature.

ture of the fluid, and this state merits the description *lattice fluid*. At 40 K, the six inner spots are strongly smeared in the azimuthal angle, but there is still significant intensity at the four outer spots. In (b) for 65 K, the pattern is primarily a ring with scarcely any modulation visible but weak spots remain at the positions of the graphite reciprocal lattice vectors. In fact the ring pattern in (b) is very similar to that shown in (c) for the same average coverage on the smooth surface at 30 K (3 K above its melting temperature).

The patterns are similar for $\rho=7/14$, where again some modulation is evident for the corrugated-substrate case at 10 K above the melting temperature. The radius of the first ring in the $S(\mathbf{q})$ pattern depends only weakly on the density, as expected for a pair correlation function with a nearest-neighbor peak determined mainly by the length scale of the intermolecular potential, rather than by the average density. With an uncertainty of ± 0.05 Å^{-1} set by the grids of the computation, the first ring on the smooth surface for $\rho=7/14$ occurs at $q\cong 1.50$ Å^{-1} and for $\rho=10/14$ at $q\simeq 1.55$ Å^{-1}.

In summary, we have found that the effect of the corrugation on the structure of the fluid persists up to a temperature of about 60 K, that is 30 K above the melting point or twice the barrier height of 30 K (Ref. 18) in the corrugation of the holding potential.

III. ISOSTERIC HEAT OF ADSORPTION

There still are not conclusive tests of the interaction models for N$_2$/graphite. The calculated melting temperature of the submonolayer commensurate solid is[3] very sensitive to the inclusion or omission of the McLachlan approximation[16] to the substrate-mediated interaction. The McLachlan term contributes approximately 15% of the lateral cohesive energy, and when it is included in the model the melting temperature is 34 K rather than the observed 47 K. Thus we seek measures of the cohesive energy of the monolayer accurate to better than 10%. This is known to be a challenging task as the most direct measures available for the monolayer cohe-
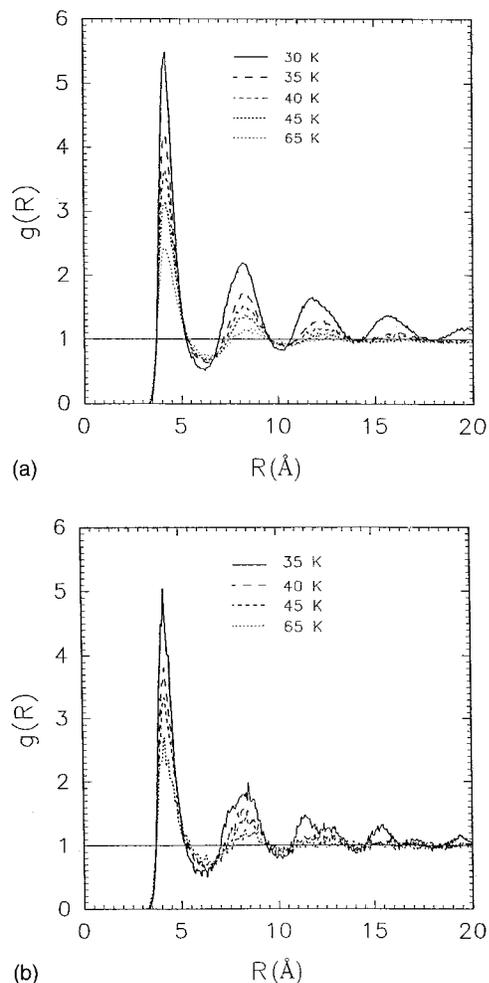
FIG. 4. The pair distribution functions $g(r)$ for the $\rho=0.5$ fluid film at different temperatures. The function is normalized to the overall average density. (a) On a model uncorrugated graphite surface. (b) On a corrugated graphite surface.

sive energy are based on determining the 2D heat of sublimation by helium atom scattering[8,9] and the values are rarely given to better than 15%.

The measurements of Piper et al.[17] of the heat of adsorption of N_2 on Grafoil at 79.3 K as a function of coverage provide a basis for checking the intermolecular potentials used in the simulations. They have reported both the isosteric heat of adsorption and integral heat of adsorption as a function of coverage in the range of 0.02–1.3 monolayers.

The molar isosteric heat of adsorption, q_{st}, may like heats of vaporization be determined from vapor pressure measurements by a Claussius–Clapeyron-type equation,

$$q_{st}=-R\left(\frac{\partial \ln p}{\partial \frac{1}{T}}\right)_{\Theta},\tag{4}$$

where p is the vapor pressure in the 3D gas, T is the temperature, and the coverage Θ is the 2D number density n measured in units of a commensurate N_2/graphite monolayer: $\Theta=n/0.0636 \text{ Å}^{-2}$. By some standard thermodynamical manipulations one may derive an alternative expression for q_{st}, which is more convenient in a simulation,

$$q_{st}=h_g-\left(\frac{\partial(nu)}{\partial n}\right)_T\tag{5}$$

using the molar internal energy u of the adsorbed molecules and the molar enthalpy h_g of the coexisting 3D gas. They may be written as

$$u=u_{kin}+u_{pot},$$
$$h_g=u_{kin}+pV=u_{kin}+RT,\tag{6}$$

where we have split the internal energy u into a kinetic, u_{kin}, and potential energy, u_{pot}, part and assumed the gas phase to be ideal. In the classical approximation the kinetic energies per mole are equal in the 3D gas and the adsorbed phase, so that q_{st} is given simply in terms of the potential energy as function of coverage,

$$q_{st}=u_{kin}+RT-\left(\frac{\partial(n(u_{kin}+u_{pot}))}{\partial n}\right)$$
$$=RT-\left(\frac{\partial(nu_{pot})}{\partial n}\right)_T=RT-\left(\frac{\partial(\Theta u_{pot})}{\partial \Theta}\right)_T.\tag{7}$$

That is, the isosteric heat of adsorption per molecule may be found from the molecular potential energy, when it has been determined as a function of coverage at the relevant temperature. The slope of the isosteric heat is given in terms of the 2D isothermal bulk modulus B_T by

$$\frac{\partial q_{st}}{\partial n}\bigg|_T=-\frac{1}{n^2}\left[B_T-T\frac{\partial B_T}{\partial T}\bigg|_n\right].\tag{8}$$

This form exhibits the relation of the slope to the monolayer equation of state and demonstrates that different features are probed at high and low coverage. The negative slope at high coverage indicates the slope is dominated by the B_T term, while the positive slope at low coverage is set by the (usual case) positive temperature derivative of the second virial coefficient.

The experimental data are reproduced in Fig. 6. The large values of q_{st} at the lowest coverages are attributed to some heterogeneity in the energy of the adsorption sites of the Grafoil.[17] One set of data shows a sharp feature near monolayer completion, a signature of the transition from a two-dimensional fluid state to a registered $\sqrt{3}\times\sqrt{3}$ two-dimensional solid phase. Above monolayer completion both sets of data approach the ordinary heat of vaporization for N_2. The nearly linear part in the intermediate range of coverages reflects the intermolecular interactions in the system. Extrapolation of the isosteric heat of adsorption to zero coverage gives the adsorption energy of a single molecule. This extrapolation is somewhat uncertain due to the heterogeneity at small coverages. The authors extrapolate to a value of 1250 K at zero coverage; this seems to be based on a tangent to the curve at a coverage of ≈ 0.18 which still seems to be in a range where the heterogeneity affects the curve. The slope of the tangent at this coverage is ≈ 199 K. If the extrapolation is based on a tangent to the curve at a coverage of $\rho=0.5$, then the isosteric heat of adsorption at zero coverage is 1203 K and the slope of the tangent is 379 K. This shows
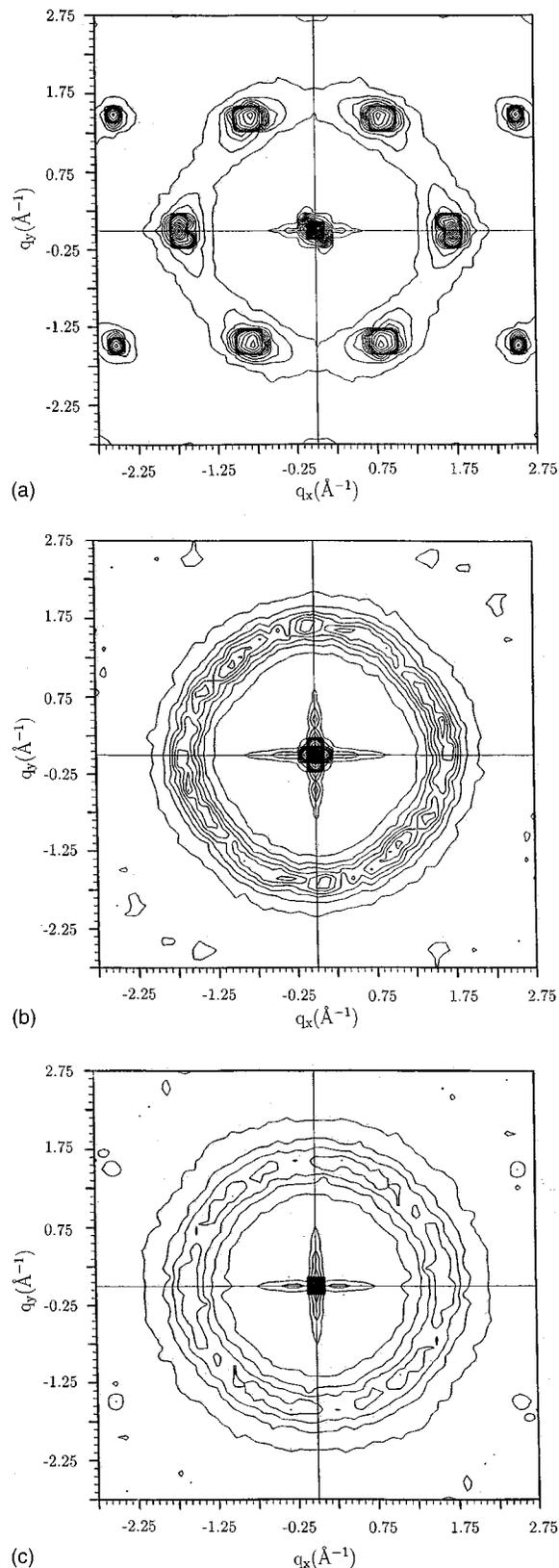
FIG. 5. The 2D structure factor for the $\rho=10/14$ fluid. (a) Corrugated graphite surface at 35 K. (b) Corrugated surface at 65 K. (c) Model uncorrugated graphite surface at 30 K.

that the determination of the slope from the experimental data is quite uncertain which is unfortunate, since we need the slope to test the model for the intermolecular interactions.
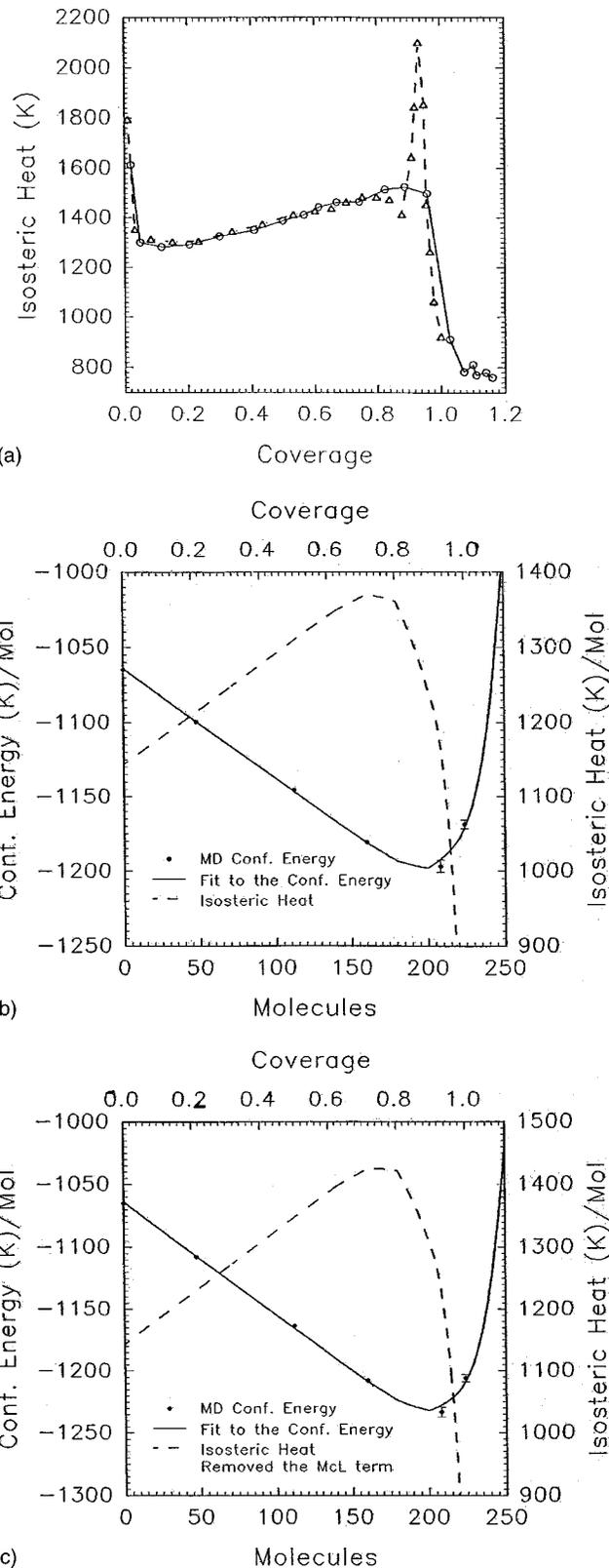

FIG. 6. (a) Plot of the experimental isosteric heat data by Piper *et al.* (Ref. 17) as a function of coverage in units of monolayer coverage. The symbols denote two independent series of measurements and the lines are drawn as a guide for the eye. Note that the Θ variable used in the experimental work is identical to the ρ variable used in this paper. (b) Plots of calculated configurational potential energy for a molecule and the isosteric heat of adsorption with the McLachlan term included. (c) Plots of the configurational potential energy for a molecule and the isosteric heat of adsorption without the McLachlan term.

TABLE I. Comparison between experimental and calculated isosteric heats of adsorption for nitrogen molecules adsorbed on the basal plane of graphite.

	Experiment			Simulation	
	Tangent at $\Theta=0.18$	Tangent at $\Theta=0.5$	Fit[a]	With surface mediation	No surface mediation[b]
$q_{st}\|_0$ (K)	1251	1202	1200 ± 25	1145	1145
Slope (K)	199	379	375 ± 25	327	394
Position of maximum		$\Theta=0.76$[c]		$\Theta=0.8$[c]	

[a]Linear fit to the data of Piper *et al.* (Ref. 17) by Talbot *et al.* (Ref. 22).
[b]Talbot *et al.* (Ref. 22) report values 1195 K and 390 K for a very similar model.
[c]Note that the Θ variable in the table is the same as ρ variable in this paper.

The simulation results are shown in Figs. 6(b) and 6(c). Both the average molecular potential energy u_{pot} and the isosteric heat of adsorption q_{st} are shown as functions of coverage. The simulation data for u_{pot} were fitted to a polynomial of the form,

$$u_{pot}=a_0+a_1\Theta+a_{13}\Theta^{13}, \qquad (9)$$

and q_{st} (in Kelvin) was then calculated from

$$q_{st}=79.3-(a_0+2a_1\Theta+14a_{13}\Theta^{13}). \qquad (10)$$

The coverage-dependent q_{st} has been calculated for models with and without the McLachlan term in the intermolecular potential. The results are very similar to the experimental data except for the apparent heterogeneity effects at low coverages and the sharp feature associated with monolayer solidification. The calculated q_{st} is linear in coverage over a wide range, which enables a precise determination of the slope $-2a_1$ and the intercept $79.3-a_0$ at zero coverage. The results of the fits to the simulation data are given in Table I.

The entries for $q_{st}\|_0$ agree to within 10%. Since the lateral-average component of the holding potential model is based on an empirical construction which could be fine-tuned to get even closer agreement, and the monolayer simulations have not proven to be sensitive to this part, we do not discuss it further. The considerable uncertainty in the experimental determination of the slope limits the conclusiveness of tests of the model of the lateral interaction. The slope fitted at $\Theta=0.5$ lies between the results for the model with and without the McLachlan term. In terms of the overall fit by Talbot *et al.*,[22] the slope without the McLachlan term is just within the assigned uncertainty while that with the McLachlan term lies at the two-standard-deviation limit. This comparison and analysis of gas–surface virial coefficients[23] confirm that adsorption-induced modifications of the intermolecular potential indeed should be included in a realistic model of the interaction. In the simulations, the McLachlan term constitutes about 15% of the total intermolecular potential energy. Interpolating between the model entries in Table I suggests that scaling it down by a factor of 3 would lead to a very good fit of the isosteric heat data. This also would do much to improve the agreement of the calculated melting temperature with experiment for submonolayer N_2/graphite.
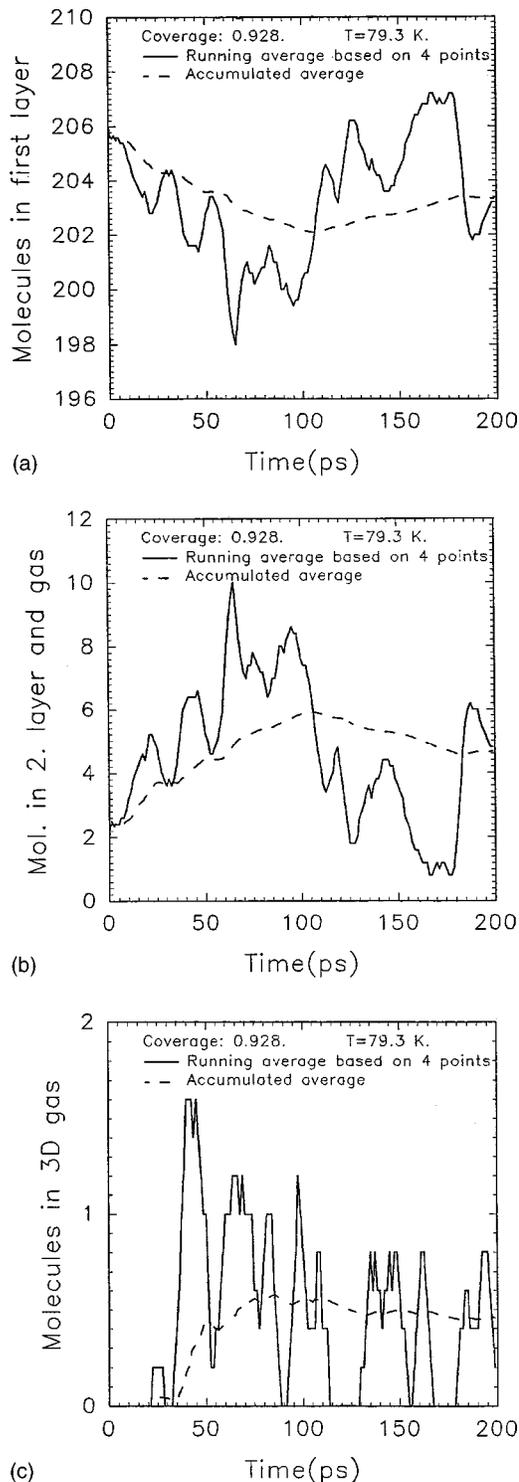

FIG. 7. Distribution of molecules over the first layer, the second layer, and the 3D gas phase in a simulation of the $\rho=13/14$ film. The total number of molecules in the simulation is 208. (a) The number of molecules in the first layer on the substrate. (b) The number of molecules in the second layer. (c) The number of molecules in the 3D gas phase.

The position of the maximum in the experimental data and in the simulations agree rather well according to Table I, and the simulations have shown that molecules are being promoted to a second layer or the 3D gas phase at this maximum. This phenomenon has been investigated in long simulations. Molecules at a distance of 0–6 Å from the surface

are defined to be in the first layer, molecules at a distance between 6 and 8 Å in the second layer and molecules above 8 Å in the 3D gas phase. In order to establish equilibrium between adsorbed molecules and molecules in the 3D gas phase, all molecules are reflected elastically at a ceiling 12 Å above the surface and sent back towards the surface. At that distance the interaction between molecule and substrate is practically zero. An example of the distribution of molecules between the three regions is shown in Fig. 7 for a $\rho = 13/14$ ($\rho = 0.928$) monolayer film. At monolayer completion there are 224 molecules so at this coverage there will be 208 molecules. In the figures we have shown the time variation of the populations over a 200 ps time span after the system has been equilibrated for ≈ 2000 ps; both a running average and an accumulated average of the number of molecules are shown. The former emphasizes the fluctuations in the populations and the latter indicates the degree of equilibrations. Equilibrium seems to be reasonably well established as the accumulated averages seem to level out to a horizontal curve. The data for $\rho = 13/14$ at 79.3 K show that ≈ 203 molecules (97.6%) are in the first layer, ≈ 5 molecules (2.4%) in the second layer and ≈ 0.5 molecules (0.2%) in the 3D gas phase. For $\rho = 1$ at 79.3 K with 224 molecules, the simulation has $\approx 95\%$ of the molecules in the first layer, 4.9% in the second layer and 0.5% in the 3D gas phase.

In general, a good agreement is found between experimental and calculated isosteric heats of adsorption. The heat of adsorption at zero coverage differs only by a few percent. In order to match the slope in the experimental data at a density $\rho = 0.5$ with our simulations, it seems necessary to reduce the magnitude of the McLachlan term consistent with our conclusions from the melting transition simulations.

IV. CONCLUSION

The comparison between calculated and measured isosteric heats of adsorption in fluid films of nitrogen molecules on graphite at 79.3 K has shown that the McLachlan mediation of the intermolecular potential should be included in a model of the interactions; its magnitude, however, may have been overestimated in the present model. This supports the studies of the melting transitions in submonolayer films, where it was shown that the McLachlan term should be reduced from its current 15% of the intermolecular energy to $\approx 3\% - 4\%$. At least part of that reduction may be achieved by an adjustment of the position of the mirror plane for electric mirror charges in the graphite substrate. Alternatively, there are missing a term in our potential model for the system that may offset the McLachlan term like when we discovered[3] that it was important to include the effect of the asymmetric charge distribution in graphite in the interaction model to obtain a better representation of the corrugation in the holding potential. At this point we are unable to decide between the two possibilities.

The corrugation in the holding potential induces some hexagonal structure in the fluid, not seen in films on a model uncorrugated graphite surface, at temperatures as high as 60 K, ≈ 30 K above the melting point and about twice the height of the potential barrier in the corrugation.

It has been demonstrated that this model of the system has the feature that it is transformed from being an incipient triple point system to a normal triple point system, when the corrugation in the holding potential is removed.

[1] D. Marx and H. Wiechert, Adv. Chem. Phys. **95**, 213 (1997).

[2] R. D. Etters, B. Kuchta, and J. Belak, Phys. Rev. Lett. **70**, 826 (1993); M. Roth and R. D. Etters, Phys. Rev. B **44**, 6581 (1991); R. D. Etters, M. W. Roth, and B. Kuchta, Phys. Rev. Lett. **65**, 3140 (1990).

[3] F. Y. Hansen and L. W. Bruch, Phys. Rev. B **51**, 2515 (1995).

[4] F. Y. Hansen, L. W. Bruch, and H. Taub, Phys. Rev. B **52**, 8515 (1995).

[5] *Phase Transitions in Surface Films 2*, edited by H. Taub, G. Torzo, H. J. Lauter, and S. C. Fain, Jr. (Plenum, New York, 1991).

[6] G. S. Leatherman and R. D. Diehl, Langmuir **13**, 7063 (1997).

[7] C. Ramseyer, C. Girardet, F. Bartolucci, G. Schmitz, R. Franchy, D. Teillet-Billy, and J. P. Gauyacq, Phys. Rev. B **58**, 4111 (1998).

[8] A. Marmier, C. Ramseyer, P. N. M. Hoang, C. Girardet, J. Goerge, P. Zeppenfeld, M. Büchel, R. David, and G. Comsa, Surf. Sci. **383**, 321 (1997).

[9] P. Zeppenfeld, R. David, C. Ramseyer, P. N. M. Hoang, and C. Girardet, Surf. Sci. **444**, 163 (1999).

[10] K. W. Herwig, Z. Wu, P. Dai, H. Taub, and F. Y. Hansen, J. Chem. Phys. **107**, 5186 (1997).

[11] J. Ellis, A. P. Graham, and J. P. Toennies, Phys. Rev. Lett. **82**, 5072 (1999), and references therein.

[12] F. Y. Hansen and L. W. Bruch, Phys. Rev. B (in press).

[13] K. J. Niskanen and R. B. Griffiths, Phys. Rev. B **32**, 5858 (1985); K. J. Niskanen, *ibid.* **33**, 1830 (1986); L. M. Sander and J. Hautman, *ibid.* **29**, 2171 (1984); A. D. Migone, M. H. W. Chan, K. J. Niskanen, and R. B. Griffiths, J. Phys. C **16**, L1115 (1983).

[14] L. W. Bruch and F. Y. Hansen, Phys. Rev. B **57**, 9285 (1998).

[15] C. S. Murthy, K. Singer, M. L. Klein, and I. R. McDonald, Mol. Phys. **41**, 1387 (1980); W. A. Steele, J. Phys. (Paris), Colloq. **38**, C4 (1978).

[16] A. D. McLachlan, Mol. Phys. **7**, 381 (1964); L. W. Bruch, J. Chem. Phys. **79**, 3148 (1983).

[17] J. Piper, J. A. Morrison, C. Peters, and Y. Ozaki, J. Chem. Soc., Faraday Trans. 1 **79**, 2863 (1983).

[18] F. Y. Hansen, L. W. Bruch, and S. E. Roosevelt, Phys. Rev. B **45**, 11238 (1992).

[19] T. T. Chung and J. G. Dash, Surf. Sci. **66**, 559 (1977); M. H. W. Chan, A. D. Migone, K. D. Miner, and Z. R. Li, Phys. Rev. Lett. **30**, 2681 (1984).

[20] B. Smit and D. Frenkel, J. Chem. Phys. **94**, 5663 (1991), have shown that the critical point for a 2D monatomic fluid depends sensitively on the cutoffs used in the potential model. In our calculation for N_2, the atom–atom interactions were cut off at 10 Å.

[21] The strong intensity at the reciprocal lattice vectors of the $\sqrt{3}$-commensurate lattice is a distinct signal from the modulation of the fluid density with fourier components of the graphite reciprocal lattice which was discussed by Talbot *et al.* (Ref. 22).

[22] J. Talbot, D. J. Tildesley, and W. A. Steele, Discuss. Faraday Soc. **80**, 91 (1985).

[23] M. J. Bojan and W. A. Steele, Langmuir **3**, 116 (1987).